

# Real-time dose prediction for Artemis missions

Shaowen Hu<sup>1,\*</sup>, Janet E. Barzilla<sup>2</sup>, Marlon Núñez<sup>3</sup>, and Edward Semones<sup>4</sup>

<sup>1</sup> KBR, Houston, TX, USA

<sup>2</sup> Space Exploration and Mission Operations, Leidos, Houston, TX, USA

<sup>3</sup> Department of Languages and Computer Sciences, Universidad de Málaga, 29016 Málaga, Spain

<sup>4</sup> Space Radiation Analysis Group, NASA Johnson Space Center, Houston, TX, USA

Received 8 July 2024 / Accepted 25 November 2024

**Abstract**—As large solar energetic particle (SEP) events can add significant radiation dose to astronauts in a short period of time and even induce acute clinical responses during missions, they present a concern for manned space flight operation. To assist the operations team in modeling and monitoring organ doses and any possible acute radiation-induced risks to astronauts during SEP events in real time, ARRT (Acute Radiation Risks Tool) 1.0 has been developed and successfully tested for Artemis I mission. The ARRT 2.0 described in this work integrates an established SEP forecasting model – UMASEP-100, further enabling real-time dose prediction for the upcoming Artemis II and following missions. With the new module linking with UMASEP-100 outputs in real time, the total BFO doses of most significant events can be communicated at the time of onset and hours before the peak. This is based on a flux-dose formula identified from comparing UMASEP-100 results with transport calculation for the events during 1994–2013 and validated with events outside that period. ARRT 2.0 also shows capability to distinguish minor events from significant ones to screen false alarms that will cause disruptions for space activities. This improvement provides additional information for operational teams to make timely decisions in contingent scenarios of severe SEP events to mitigate radiation exposure.

**Keywords:** Solar particle events / Radiation exposure mitigation / Forecasting models / Artemis missions / Operational management

## 1 Introduction

For exploration beyond the Earth's protective magnetosphere such as lunar and Mars missions, excessive radiation exposure during severe solar energetic particle (SEP) events is a concern for humans in space. The health risks due to radiation exposure include latent effects such as carcinogenesis, degenerative tissue damage, and damage to the central nervous system, and acute radiation syndrome (ARS) which consists of a group of clinically significant syndromes such as fatigue, weakness, and nausea that may manifest during missions (Cucinotta et al., 2010). To protect against these risks, one approach of the National Aeronautics and Space Administration (NASA) is to define the permissible exposure limits (PEL). Most recently, the PEL for individual crewmember's career effective radiation dose during spaceflight radiation exposure is not to exceed 600 mSv (Sv is effective dose unit by multiplying absorbed dose in Gy with quality factors associated with specific types of radiation) (National Academies of Sciences, Engineering, and

Medicine, 2021; NASA, 2023), and short-term (30 days) radiation exposure to solar particle events is limited to blood forming organ (BFO) dose 250 mGy-Eq to minimize acute effects (Gy-Eq is unit for deterministic effects by multiplying absorbed dose in Gy with relative biological effects (RBEs) associated with specific types of radiation) (NASA, 2023), with a best effort to keep the exposure as low as reasonably achievable (i.e., the ALARA principle; National Council on Radiation Protection, 2000).

To monitor the exposure astronauts receive and the possible acute effects during the upcoming Artemis missions, NASA has developed a tool ARRT (Acute Radiation Risks Tool) to enhance communication between ground operational team and the crew by using the onboard dosimeters as a data stream (Hu et al., 2020). Traditionally, the radiation exposure due to SEP events is modeled based on measurements of satellites deployed either close to the Earth or in interplanetary space, which is not applicable to interplanetary missions such as Mars mission as major part of the trajectories is far from any satellites. Using onboard dosimeters measurements to estimate radiation exposure for interplanetary missions was initially proposed in

\*Corresponding author: [shaowen.hu-1@nasa.gov](mailto:shaowen.hu-1@nasa.gov)

1970s (Wilson & Denn, 1976), and was recently implemented for the ongoing Artemis missions (Mertens et al., 2018), upon which ARRT was built. The algorithm involves a fitting procedure between the real-time vehicle dosimeter measurements and a precomputed database of dose quantities calculated from the HZETRN radiation transport code (Slaba et al., 2016; Wilson et al., 2016), considering the actual Orion Multi-Purpose Crew Vehicle (MPCV) geometry and mass distribution. The estimated organ doses at the crew locations are utilized as inputs to a set of biological response models, which predict clinically critical syndromes associated with ARS and quantify Radiation-Induced Performance Decrement (RIPD; Hu et al., 2009, 2012; Hu & Cucinotta, 2011).. This tool has been fully tested to the extent possible, given the quiet space environment, for the Artemis I mission in 2022, and will be utilized in the upcoming lunar missions.

In case of severe SEP events, the exposure and ARS effects can also be mitigated during the vehicle design process through thoughtful redistribution of stowage mass to the vehicle periphery to provide optimal radiation shielding. The NASA Space Radiation Analysis Group (SRAG) has been closely involved with the design process of the MPCV to identify locations with lower inherent shielding and attempt to improve the overall shielding concept without adding excess mass to the vehicle. If additional protection is necessary, a contingency solar storm shelter has been designated where the crew can shelter in the stowage bays of the vehicle and redistribute the mass contained within this area to reduce radiation exposure (Hu et al., 2020). An alternative sheltering scenario is also under development to redistribute mass to lower shielding locations of MPCV without limiting the activities of the crew (A. S. Johnson and D. Laramore, private communications). To make timely decisions in such situations, surveillance methods to predict and detect solar particle events are required, which should neither miss SEP events nor issue false alarms at an unacceptably high rate.

In this work, we report an upgraded ARRT version 2.0 integrated with a well-established SEP forecasting model – UMASEP-100, which makes real-time predictions of the time interval within which the >100 MeV proton flux is expected to surpass 1 proton  $\text{cm}^{-2} \text{sr}^{-1} \text{s}^{-1}$  (proton flux unit (pfu)) and the intensity of the first 3 h of the event (Núñez, 2015). Based on a correlation between the model forecasted fluxes and simulated organ doses inside MPCV in free space, the upgraded tool can perform real time dose projection for the upcoming Artemis missions, giving the total exposure information either before or shortly after the onset of an event. Combined with the organ dose estimated through the on-board dosimeter readings and the modeled set of acute risks in real time, this tool will provide essential information for operational teams to distinguish significant events from insignificant events, and to make educated decisions if crew action is necessary to shelter to reduce radiation exposure in case of severe SEP events.

This paper is organized as follows: Section 2 describes the UMASEP-100 forecasting model, Section 3 summarizes the functions of ARRT 1.0, Section 4 shows how the correlation of forecasted flux and the total BFO dose is established and validated, Sections 5 and 6 discuss the enhanced functions of the UMASEP-integrated ARRT 2.0, Section 7 presents a new validation of ARRT organ dose algorithm based on this work, and Section 8 presents conclusions.

## 2 UMASEP

UMASEP-100 is a tool for predicting the occurrence of >100 MeV energetic solar proton events (ESPE), the first 3 h of the >100 MeV integral proton flux, and the fluence of 118 MeV (Núñez, 2015). The preliminary forecast functionality of UMASEP-100 is divided into the Well-Connected Prediction (WCP) and Poorly-Connected Prediction (PCP) models. The WCP-100 model assesses the relationship between time series GOES SXR (soft X-ray) emissions and an increase in GOES differential proton flux. It assumes that certain events at the Sun (i.e., in terms of SXR fluxes) are lag-correlated with a process that will accelerate particles that could arrive at Earth through a magnetic connection, producing a rapid increase in differential proton flux values in the near-Earth environment. Evidence of a magnetic connection is found when this model detects a large lag-correlation, which is the number of cause-consequence pairs. A cause-consequence pair is detected when a sequence of large 5-min slopes of differential particle channel fluxes is preceded by a sequence of large 5-min slopes of SXR fluxes. If there is evidence of a magnetic connection and an SXR flare has recently occurred whose peak has surpassed a threshold of  $9 \times 10^{-5} \text{ Watt/m}^2$ , a well-connected SEP event prediction is issued. To enhance the model's ability to provide advance warning of an SEP event, the WCP-100 model has recently been updated to include the Advanced Composition Explorer (ACE) Electron Proton Alpha Monitor (EPAM) electron fluxes with energies of 0.175–0.375 MeV in the lag-correlation analysis. Alternatively, the PCP-100 model compares the characteristics of the current event to similar historical events to determine if it is more likely to surpass the SEP threshold or return to background levels. As this model is intended to detect an event when there is no magnetic connection between the parent event and the observer, it only analyzes the evolution of in situ protons.

Preliminary warnings from both the WCP-100 and PCP-100 models are processed to decide if an alert will be issued, with preference given to the WCP-100 model. The alert also includes the maximum >100 MeV integral proton flux and the fluence of 118 MeV for the next 3 h, which are predicted using empirical models and formulas that were constructed using machine learning and linear log-log regression techniques over Solar Cycles (SC) 23–25 data, respectively. The calibration of all the parameters and thresholds is carried out by optimizing the Probability of Detection (POD) and False Alarm Ratio (FAR) using historical data. UMASEP-100 v1.3 was validated with data from January 1994 to September 2013 (Núñez, 2015), obtaining a POD of all >100 MeV SEP events of 80.85%, a FAR of 29.62%, and an average warning time of 1 h and 6 min. Since 2010, NASA's integrated Space Weather Analysis system (ISWA) and the European Space Weather Portal redistributes UMASEP-100's forecasts, which have obtained successful results on an operational level.

## 3 ARRT

ARRT 1.0 is developed specifically for the ongoing Artemis missions aiming to send astronauts back to the Moon. During a space flight mission, ARRT will be run at the Mission Control

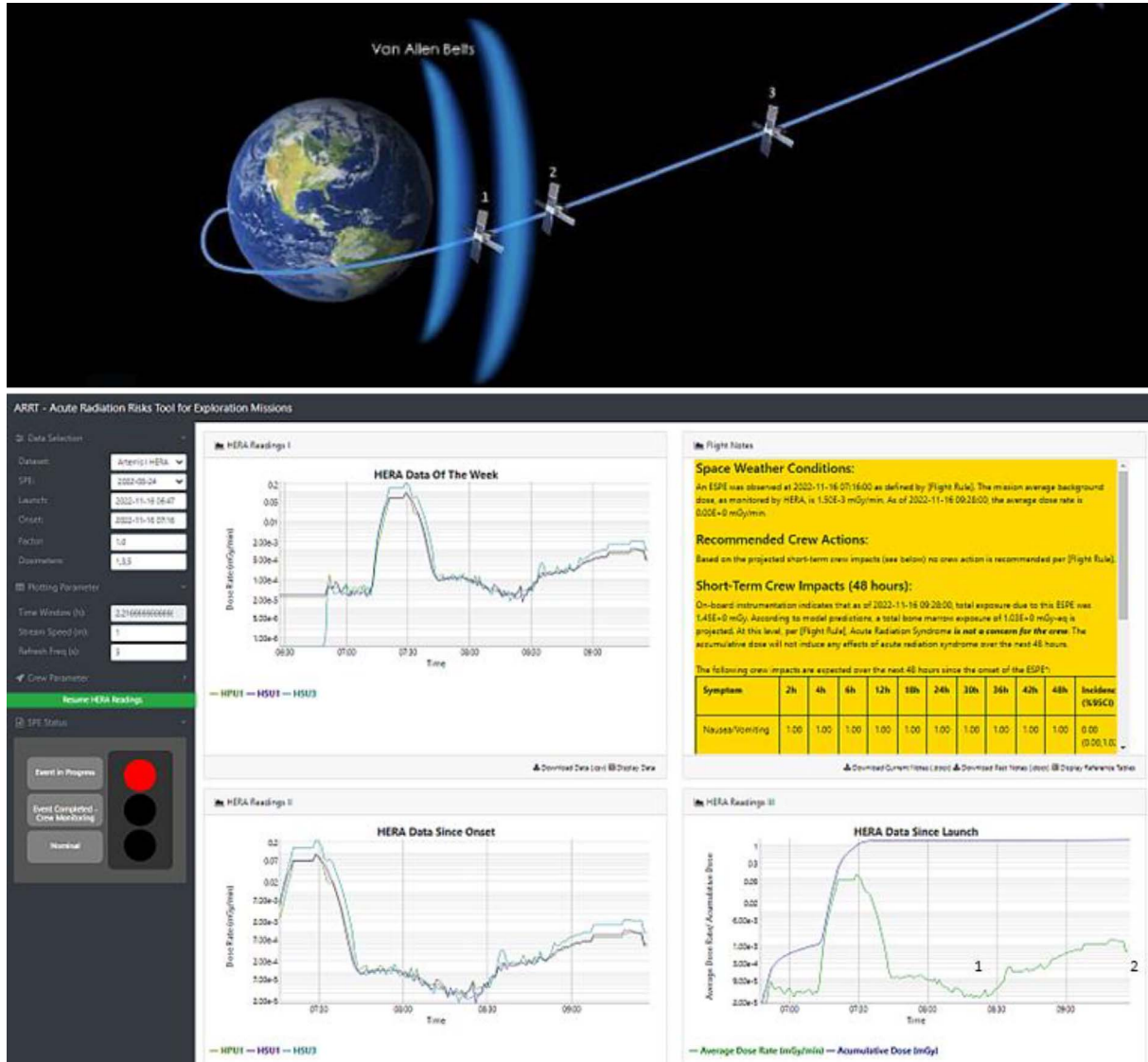


**Figure 1.** Schematic trajectory of Artemis I passing through the Van Allen Belts (top, courtesy to NASA) and rewind study of ARRT 1.0 (bottom). The average HERA dose rates corresponding to points 1 and 2 in the top trajectory figure are denoted in the right bottom panel in the ARRT interface. For description of the components of ARRT 1.0 interface see the text and the previous report (Hu et al., 2020).

Center (MCC) at Johnson Space Center of NASA, and all its output will be automatically produced at the telemetry time cadence of the vehicle dosimeter measurements, which is anticipated in the range of 15–30 min and may be changed for future missions. The operationally useful functions of the tool include rendering and plotting the dosimeter readings, detecting the onset and end of an event, calculating, and plotting the relevant organ dose quantities, triggering the ARS biological models if threshold is reached, and generating drafts of flight notes to facilitate communication of mitigation response within Flight Control Team (FCT) (Hu et al., 2020).

These functions can be demonstrated with an ARRT snapshot when Orion MPCV passed the Van Allen belt shortly after the Artemis I launch (Fig. 1). After this long-anticipated mission was finally launched on 06:47:44 (UTC) 2022-11-16, ARRT received the dose rate readings of HERA HPU1, HSU1 and HSU3 since 06:50 at 1-min interval (Fig. 1; Stoffle

et al., 2023). Before the spacecraft reached the edge of belt zone (at 07:12), the average HERA dose rates were around 0.15  $\mu\text{Gy}/\text{min}$ , and the SPE status was “Nominal” as the threshold of an ESEP event is defined as 1.5  $\mu\text{Gy}/\text{min}$  for ARRT. At 07:16, ARRT detected twice the elevated dose rates above the threshold as the spacecraft crossed well into the belt zone, and changed the SPE status to “Event in Progress”, triggered the codes to do organ dose calculation and acute risk modeling, and expanded the flight note to show information relevant to an SEP event (Fig. 1). At 07:41, the spacecraft nearly crossed the inner proton belt, and the average dose rate dropped below the threshold and never rose above it after that, though there were elevation when passing through the outer electron zone. Because the dwelling time to separate two events was defined as 2 h (Hu et al., 2020), the “event” was considered as in progress till 09:40. The total BFO dose at this point was 1.11 mGy-Eq, so all estimated acute effects were negligible,



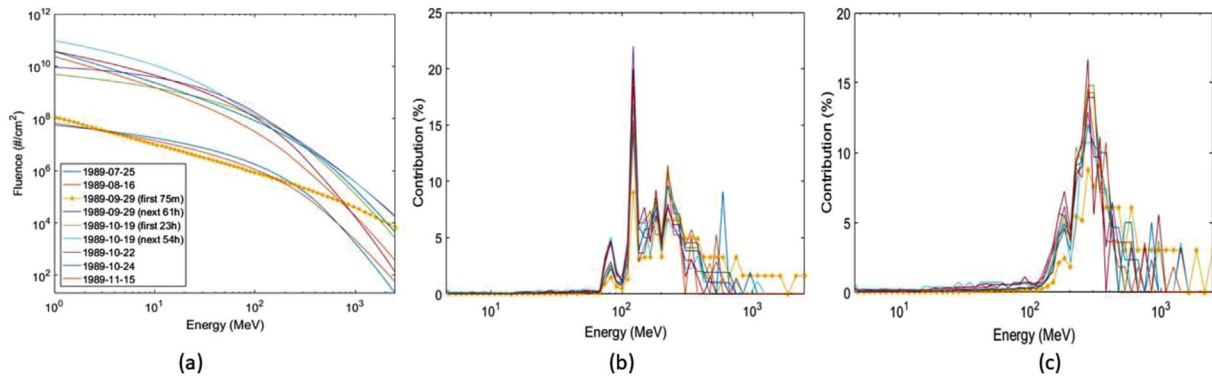


**Figure 2.** Segmental spectral contributions of protons to the HPU1 doses and BFO doses inside MPCV. (a) Band spectra of 9 subevents in 1989 (Raukunen et al., 2018). (b) Contributions of protons at different energies to the total HPU1 doses of the 9 events. (c) Contributions of protons at different energies to the total BFO doses for a FAX phantom at seat 1 of the 9 events. (a) and (b) are adapted from Figure 3 in Hu et al. (2020).

and no crew monitoring phase was triggered (Hu et al., 2020). After this time point, ARRT switched back to and stayed as “Nominal” status, as no SPE event was encountered during this 26-day mission beyond LEO (Low Earth Orbit). It should be noted that the triggering of ARRT in the belt zone was suppressed in Mission Control so as not to alarm the console operations team.

#### 4 Correlation between UMASEP-100 predicted fluxes and event BFO doses

Utilizing UMASEP-100 to upgrade ARRT is based on a previous finding that proton fluxes with energies  $>100$  MeV are the most relevant to the absorbed doses for detectors/crew inside the MPCV (Hu et al., 2020). We conducted transport calculations to investigate the segmental spectrum contribution to silicon doses at the locations of HERA dosimeters in MPCV, with the Band spectra in the energy range 0.01–2500 MeV for nine subevents in 1989 (Hu et al., 2020). Here we extend the analysis for a FAX phantom (Slaba et al., 2010) at seat 1. As shown in Figure 2, the contributions to HPU1 doses mainly come from the protons in the energy range 70–300 MeV, with a peak at 122 MeV. Assuming a phantom is located at seat 1, with additional shielding of human tissues like skin and muscle, the BFO doses are contributed mainly from protons in the energy range 150–400 MeV, and peak shifts to around 275 MeV (Fig. 2). Clearly the protons with energies  $<100$  MeV have only very minor impacts for internal organs such as BFO inside MPCV. Nevertheless, the detailed contribution to resulted doses is highly dependent upon the shape of the spectrum. For example, for the first 75 min of the 29 September 1989 event which has the hardest spectrum among these events, the contribution of the protons with energy  $>289$  MeV to HPU1 dose is around 46%, while the corresponding contributions for other events are much smaller (Hu et al., 2020).

To identify the correlation between the UMASEP-100 predicted flux and BFO dose inside MPCV, we conducted two independent calculations. First, we ran UMASEP-100 v3.4 for the events listed in Table 1 of the reference (Núñez, 2015) to

get the predicted fluxes at ST + 3 h (3 h after the Starting Time (ST)); Then we did transport calculation to get BFO dose for crew inside MPCV, by using a recent cross-calibrated uniform data set from the Geostationary Operational Environmental Satellite (GOES) measured solar proton fluxes during 1986–2019, with an energy range 10–1000 MeV (Hu & Semones, 2022a, 2022b). With segmental spectra (Hu et al., 2016) of 5-min cadence generated from the fluxes as a boundary condition, and material and shielding thicknesses determined by ray tracing the computer-aided design (CAD) model of the MPCV for FAX phantom at seat 1, transport calculations through the vehicle are performed by a numerical solution of the one-dimensional Boltzmann transport equation using the HZETRN2015 code (Slaba et al., 2016; Wilson et al., 2016). The resultant data set contains BFO dose rates spanning uniformly from 1986 to 2019, with a 5-min cadence.

The event total BFO dose and duration are determined by an algorithm to automatically calculate the background and to determine the onset and end of an event (Hu et al., 2020; Hu & Semones, 2022b). A 1-day window is selected to calculate mean dose rate and the number of point dose rates below the mean dose rate. If the number of point dose rates below the mean dose rate is less than 55% of the total number of points in this time window, it is certain that there is no solar particle event (SPE) during this window and the calculated mean is considered as the background dose rate. Otherwise, the time window shifts 1 day or additional days ahead until the condition is satisfied. A value of 1.5 times the background is used as the threshold. If fluxes of 6 consequent time points (i.e., 0.5 h) are above threshold, the first point is considered as the start of an event. If fluxes of 24 consequent time points (i.e., 2 h) are below the threshold, the first point is considered as the end of an event, which defines the duration of the event. This algorithm has been verified with recorded proton data during 1986–2019, and the identified events are close to the lists of the National Oceanographic and Atmospheric Administration (NOAA) SEP events and the Solar Energetic Particle Environment Modelling (SEP-EM) reference events (Hu & Semones, 2022b)

With this procedure, 61 SEP events are identified from the modeled BFO dose data set during 1994–2013, and 44 of them

**Table 1.** List of SPEs used to derive correlation formula between UMASEP predicted flux and BFO dose inside MPCV.

| SPE number | Event start time (ST) by SWPC | GOES proton flux (ST + 3 h) | UMASEP 3.4 proton flux (ST + 3 h) | Start time (ST) by BFO dose | $\Delta$ ST (m) | BFO dose (mGy-Eq) | Duration (d) |
|------------|-------------------------------|-----------------------------|-----------------------------------|-----------------------------|-----------------|-------------------|--------------|
| 1          | 1997-11-04 07:25              | 1.93                        |                                   | 07:20                       | 5               | 0.13              | 0.24         |
| 2          | 1997-11-06 12:45              | 46.3                        | 4.07                              | 12:25                       | 20              | 5.77              | 1.34         |
| 3          | 1998-04-20 17:10              | 1.83                        | 1.63                              | 21:55                       | -285            | 0.84              | 1.3          |
| 4          | 1998-05-02 14:05              | 5.36                        | 7.32                              | 13:55                       | 10              | 0.66              | 0.62         |
| 5          | 1998-05-06 08:30              | 1.9                         | 4.88                              | 08:20                       | 10              | 0.16              | 0.27         |
| 6          | 1998-08-24 23:10              | 2.94                        | 3.25                              | 22:45                       | 25              | 0.53              | 0.83         |
| 7          | 1998-09-30 15:20              | 2.81                        | 1.63                              | 14:40                       | 40              | 0.22              | 0.44         |
| 8          | 1998-11-14 07:55              | 5.28                        | 2.44                              | 07:55                       | 0               | 0.29              | 0.38         |
| 9          | 2000-06-10 17:50              | 0.41                        | 1.63                              | 17:45                       | 5               | 0.03              | 0.09         |
| 10         | 2000-07-14 10:40              | 374                         | 316.26                            | 10:30                       | 10              | 39.40             | 2.29         |
| 11         | 2000-11-08 23:55              | 311                         | 243.9                             | 23:45                       | 10              | 22.20             | 2.23         |
| 12         | 2000-11-24 17:20              | 0.58                        | 1.63                              | 16:40                       | 40              | 0.04              | 0.15         |
| 13         | 2000-11-26 16:40              | 1.07                        | 1.63                              | 15:55                       | 45              | 0.08              | 0.3          |
| 14         | 2001-04-03 01:20              | 4.52                        | 3.25                              | 01:05                       | 15              | 0.53              | 1.03         |
| 15         | 2001-04-12 13:05              | 1.05                        |                                   | 12:15                       | 50              | 0.11              | 0.36         |
| 16         | 2001-04-15 14:05              | 89.1                        | 63.41                             | 13:55                       | 10              | 13.90             | 4.22         |
| 17         | 2001-04-18 02:55              | 12.8                        |                                   |                             |                 |                   |              |
| 18         | 2001-08-16 01:05              | 26.3                        |                                   | 01:00                       | 5               | 1.48              | 1.57         |
| 19         | 2001-09-24 14:40              | 6.12                        | 3.25                              | 14:20                       | 20              | 5.43              | 2.68         |
| 20         | 2001-11-04 16:50              | 52.8                        | 43.09                             | 16:35                       | 15              | 17.80             | 2.4          |
| 21         | 2001-11-22 22:50              | 1.33                        | 1.63                              | 22:25                       | 25              | 2.49              | 1.81         |
| 22         | 2001-12-26 05:55              | 25.4                        | 7.32                              | 05:45                       | 10              | 1.56              | 0.66         |
| 23         | 2002-04-21 01:55              | 16.1                        | 17.07                             | 01:45                       | 10              | 3.20              | 2.2          |
| 24         | 2002-08-22 03:40              | 0.84                        | 1.63                              | 03:35                       | 5               | 0.07              | 0.24         |
| 25         | 2002-08-24 01:30              | 13.3                        | 16.26                             | 01:20                       | 10              | 1.25              | 0.93         |
| 26         | 2003-10-28 11:45              | 83.9                        | 86.18                             | 11:15                       | 30              | 29.90             | 2.64         |
| 27         | 2003-11-02 17:40              | 21.2                        | 26.83                             | 17:30                       | 10              | 2.67              | 1.83         |
| 28         | 2003-11-05 05:10              | 0.81                        | 1.63                              | 23:25 (-1d)                 | 345             | 0.24              | 1.11         |
| 29         | 2004-11-01 06:35              | 0.68                        | 1.63                              | 06:40                       | -5              | 0.03              | 0.06         |
| 30         | 2004-11-10 03:20              | 1.67                        | 4.88                              | 03:15                       | 5               | 0.15              | 0.36         |
| 31         | 2005-01-17 12:15              | 20                          | 1.63                              | 12:30                       | -15             | 2.44              | 1.21         |
| 32         | 2005-01-20 06:50              | 165                         |                                   | 06:45                       | 5               | 27.20             | 1.54         |
| 33         | 2005-06-16 21:25              | 2.23                        | 3.25                              | 21:20                       | 5               | 0.19              | 0.41         |
| 34         | 2005-09-08 04:05              | 1.36                        | 1.63                              | 01:55                       | 130             | 3.91              | 3.32         |
| 35         | 2006-12-07 01:15              | 3.86                        | 1.63                              | 01:00                       | 15              | 3.45              | 1.68         |
| 36         | 2006-12-13 03:00              | 81.5                        | 70.7                              | 02:50                       | 10              | 6.27              | 1.59         |
| 37         | 2006-12-14 22:55              | 1.5                         | 1.63                              |                             |                 |                   |              |
| 38         | 2011-06-07 07:20              | 4.51                        | 1.63                              | 07:35                       | -15             | 0.30              | 0.49         |
| 39         | 2011-08-04 05:10              | 1.65                        | 1.63                              |                             |                 |                   |              |
| 40         | 2011-08-09 08:25              | 0.75                        | 1.63                              | 08:15                       | 10              | 0.05              | 0.08         |
| 41         | 2012-01-23 04:45              | 2.33                        | 1.63                              | 06:50                       | -105            | 0.59              | 1.11         |
| 42         | 2012-01-27 19:00              | 11.5                        | 13.82                             | 18:35                       | 25              | 1.03              | 0.93         |
| 43         | 2012-03-07 04:05              | 4.53                        | 1.63                              | 04:00                       | 5               | 12.00             | 2.72         |
| 44         | 2012-03-13 18:10              | 1.31                        | 1.63                              | 17:45                       | 25              | 0.12              | 0.25         |
| 45         | 2012-05-17 02:00              | 10.5                        | 8.94                              | 02:00                       | 0               | 0.93              | 0.56         |
| 46         | 2013-04-11 09:40              | 1.66                        | 3.25                              | 10:05                       | -25             | 0.13              | 0.32         |
| 47         | 2013-05-22 14:55              | 3.01                        | 2.44                              | 14:25                       | 30              | 0.71              | 1.19         |

are confirmed as the same events as used in reference (Núñez, 2015). For the 3 missing events, from 2006-12-14 to 2011-08-04 events are too small to be detected by the algorithm, and the 2001-04-18 is merged in the previous event (2001-04-15) as the dwelling time between them is less than 2 h. The start times of most events by the algorithm are earlier than those defined by NOAA SWPC (i.e., the  $\geq 10$  MeV integral flux  $> 10$  pfu) (Table 1), which is consistent with observations that high energy protons reach the Earth faster than low energy protons (Hu et al., 2016). For a few events, the BFO dose determined start times are later than the defined time (Table 1),

reflecting the complex features of SPEs in term of proton flux, energy spectrum, dose and dose rate, and duration. Of the 47 events listed in Table 1, UMASEP-100 v3.4 misses 5 in prediction, indicating an improvement from v1.3 which misses 9 (Núñez, 2015).

We have 44 events to check the correlation between proton fluxes observed by GOES and simulated BFO doses through transport calculations using MPCV as the vehicle model. With Microsoft Excel Trendline options, we find the linear and power law fittings are similar in term of  $R^2$  values, though the power law fitting is better represented in log scale (Fig. 3, left).

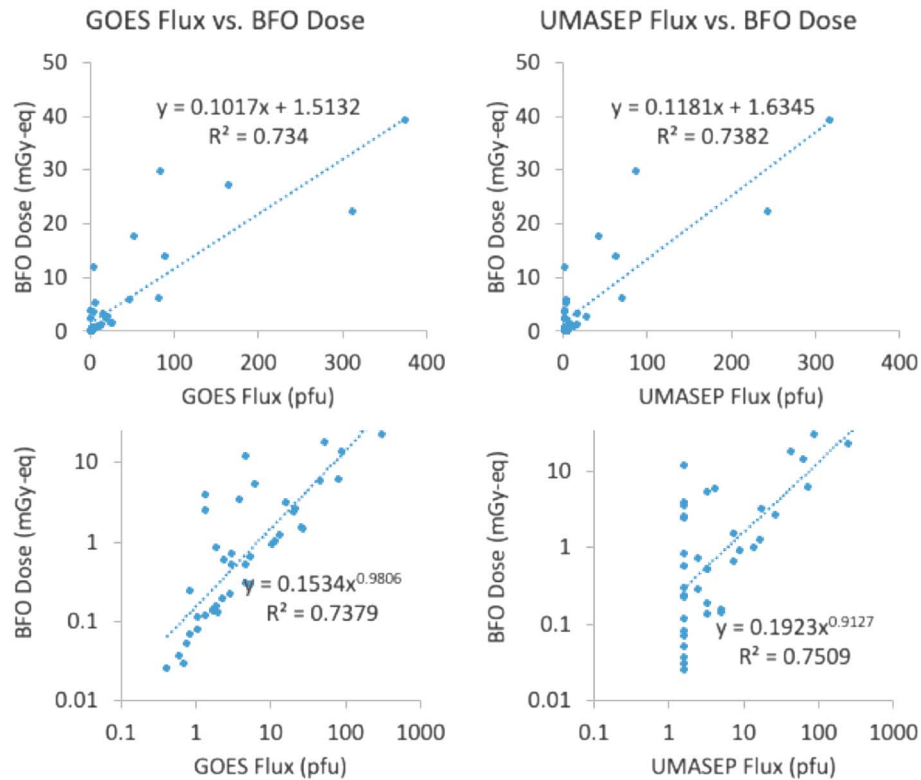


**Figure 3.** Correlation between proton flux (ST + 3 h) and BFO dose for 44 events observed with GOES (left) and for 40 events modeled with UMASEP-100 v3.4 (right). The flux-dose formulas are embedded in the plots, along with  $R^2$  values, for linear and power law fittings.

The major contributions to the residues of fitting parameters come from events with long durations (such as the events of 2003-10-28, 2012-03-07, etc.), which generally have a second peak long after the onset. For the 40 events to check between proton fluxes predicted with UMASEP-100 and BFO doses, power law fitting is also better than linear fitting, and with a bit better  $R^2$  than GOES data, respectively (Fig. 3, right). UMASEP-100 predictions have a lower limit for the forecasted proton flux (i.e., 1.63 pfu), and about half of all events are projected to this limit, with BFO doses varying from 0.03 to 12.00 mGy-Eq (Fig. 3, right bottom). This looks to be a severe limitation of the model capability. However, only 1 event of them are of significance (with BFO dose 12.00 mGy-Eq), and BFO doses of the rest are less than 5 mGy-Eq. These two sets of comparison indicate a correlation does exist between the integral proton fluxes >100 MeV shortly after the onsets and the total BFO doses for a specific spacecraft (MPCV) for historical events, and confirm the UMASEP-100's predicted proton fluxes are in good agreement with the measurements. It should be noted that the fluxes for GOES in Figure 2 and Table 1 are the measurements at exactly 3 h after the onset of each event, in contrast to the values at any other time points, as the proton flux keeps changing during the event. At the same time, the UMASEP predicted fluxes are single value for most events. Therefore, we cannot provide error bars or uncertainties for these two types of fluxes.

To choose the best flux-dose formula, we check the 2 formulas with 12 large SPEs observed by GOES but not in the period of 1994–2013 (Table 2). The start time of each event is defined when the flux of proton >100 MeV reaches 1 pfu, and

the proton flux at ST + 3 h is identified from the data files recorded by GOES 6 and 15. The 3 subsequential events in late October 1989 cannot be separated by the SPE detecting algorithm, because the BFO dose rates do not fall below the pre-event background before the subsequent events start. The event doses and durations for them are obtained by manual calculation based on their defined start times. The start times identified by the automatic algorithm are earlier than the defined ones by 5–20 min, with 2 events (Events 1 and 8) beginning exceptionally earlier (Table 2). The proton flux after the onset of any event is known to be highly dynamic, especially at the beginning hours; therefore, there is uncertainty of the proton flux at ST + 3 h chosen to evaluate the flux-dose formula.

The rapid rise phase of the largest event of 1989-10-19 leads to difficulty in selecting the better formula, as all  $R^2$  are about 0.05–0.17 if flux at ST + 3 h is used, which happens to be in a rapid rising phase and is far from the peak that UMASEP-100 model intends to predict. In fact, the first peak of this event arrives at about ST + 13 h, which is about 3 times higher than that at ST + 3 h, and the second peak arrives at about ST + 26 h, which is about 7.6 times higher (Table 2). If flux at ST + 13 h is used, the  $R^2$  value for the better fit of GOES flux-dose formulas is 0.54, and for UMASEP formulas is 0.48; If flux at ST + 26.3 h is used, the  $R^2$  value for the better fit of GOES flux-dose formulas is 0.91, and for UMASEP formulas is 0.88 (Fig. 4). As the proton flux UMASEP-100 predicts intends to be the peak of the event (Núñez, 2015), and power law fit is worse than the linear fit for strong fluxes, the linear fit flux-dose formula for UMASEP modeling is chosen to incorporate the UMASEP-100 model into ARRT.

**Table 2.** List of SPEs used to validate the flux-dose correlation formula.\*

| SPE number | Event start time (ST) | GOES proton flux (ST + 3 h) (pfu)                  | Event start time by BFO dose | $\Delta$ ST (m) | BFO dose (mGy-Eq) | Duration (d) |
|------------|-----------------------|--|------------------------------|-----------------|-------------------|--------------|
| 1          | 1989-08-12 19:25      | 4.8  | 18:35                        | 50              | 4.11              | 1.92         |
| 2          | 1989-08-16 1:40       | 53.6   | 1:25                         | 15              | 8.23              | 3.04         |
| 3          | 1989-09-29 12:00      | 263.0  | 11:40                        | 20              | 51.80             | 5.47         |
| 4          | 1989-10-19 13:05      | 75.3 (215.0 at ST + 13 h,<br>569.0 at ST + 26.3 h) | 12:55                        | 10              | 75.20             | 3.25         |
| 5          | 1989-10-22 18:05      | 175.0  |                              |                 | 30.40             | 2.01         |
| 6          | 1989-10-24 18:25      | 128.0  |                              |                 | 29.50             | 6.17         |
| 7          | 1990-05-24 21:15      | 15.7   | 21:00                        | 15              | 6.86              | 5.93         |
| 8          | 1991-03-23 12:25      | 4.7  | 5:00                         | 445             | 5.81              | 1.92         |
| 9          | 1991-06-11 2:50       | 12.6   | 2:45                         | 5               | 5.68              | 1.94         |
| 10         | 1991-06-15 8:45       | 45.4   | 8:30                         | 15              | 5.93              | 2.33         |
| 11         | 1992-11-02 3:25       | 78.0   | 3:20                         | 5               | 8.63              | 1.69         |
| 12         | 2017-09-10 16:30      | 57.5   | 16:10                        | 20              | 10.90             | 2.23         |

\* Fluxes at the first and second peaks of the 1989-10-19 event are also listed and used in analysis.

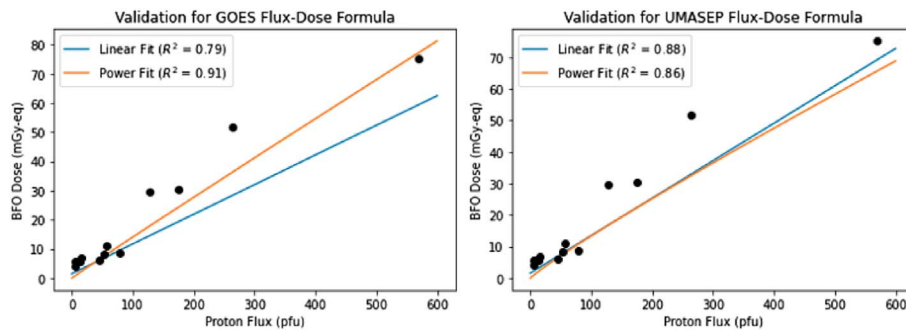


**Figure 4.** Validation of the flux-dose formulas with GOES observed proton fluxes and calculated event BFO doses. The flux for the event 1989-10-19 is at ST + 26.3 h, and the rest are at ST + 3 h.

## 5 UMASEP-integrated ARRT

ARRT 2.0 keeps all functions of the previous version, i.e., rendering and plotting the dosimeter readings, detecting the onset and end of an event, calculating and plotting the relevant organ dose quantities, triggering the ARS biological models if threshold is reached, and generating flight notes to facilitate communication of mitigation response within the Flight Control Team (FCT) (Hu et al., 2020), but adds a module to interact with UMASEP-100 model. In addition, a calibrated GOES dataset is added, which is obtained by calibrating the effective energies of various proton channels of GOES 6 to 16 with modeled Ground Level Enhancements (GLEs) spectra based on satellites measurements and ground neutron monitors measurements (Hu & Semones, 2022a, 2022b). This is a uniform data set for near Earth space proton fluxes for the period 1986–2022 with an energy range from 10 to 1000 MeV. With segmental spectra (Hu et al., 2016) of 5-min cadence generated from the fluxes as a boundary condition and material and shielding thicknesses determined by ray tracing the computer-aided design (CAD) model of the MPCV for Artemis II (with six HERA sensors), transport calculations through the vehicle are performed by a numerical solution of the one-dimensional Boltzmann

transport equation using the HZETRN2015 code (Slaba et al., 2016; Wilson et al., 2016). The resultant data set contains dose rates for the six dosimeters spanning uniformly from 1986 to 2022, with a 5-min cadence.

For historical events, UMASEP-100 v3.4 was run at Community Coordinated Modeling Center (CCMC, <https://ccmc.gsfc.nasa.gov/>) server for the events listed in Table 1, as well as known events after that period. The predicted fluxes of proton with energy >100 MeV were retrieved from the output files along with the issue time tag and were assigned zero if there were no prediction. A continuous flux data set with 5-min cadence was obtained from GOES for the period 1994–2013, and yearly flux data sets for 2017, 2021 and 2022 were obtained in the same way, as no significant SPE is recorded by GOES in near Earth space in other years (i.e., 2014–2016, 2018–2020) since 1994, the earliest time UMASEP-100 can acquire recorded data to run on the server. Observed proton integral fluxes are obtained from National Centers for Environmental Information website (<https://satdat.ngdc.noaa.gov/sem/goes/data/avg/>) for GOES 8 to 15, and from the ISWA – HAPI Server at NASA Goddard Space Flight Center (GSFC) (<https://iswa.gsfc.nasa.gov/IswaSystemWebApp/hapi/>) for GOES 16, all with a 5-min cadence.



For real time data stream, 3 days UMASEP-100 model outputs are retrieved from the CCMC website updating every 5 min; integral flux for proton with energies >10 MeV and >100 MeV are retrieved from SWPC NOAA website at the same cadence. As meaningful real-time HERA data will not be available until Artemis II starts their journeys in space, a real-time data set linking with the databases of International Space Station (ISS) instruments are used instead, which include dose rates measured by Radiation Assessment Detector (RAD) and Artemis-HERA on Space Station (AHOSS) (Hu et al., 2020). The dose rates in the record uniformly populate ARRT from their starting service time to the present time, with a 1-min cadence. As SRAG will maintain active instrumentation data for the future Artemis missions in a similar manner as for ISS, the real-time onboard data set can be easily migrated in ARRT.

A plot showing the GOES observed proton flux and UMASEP-100 predicted flux is added to ARRT 2.0 interface (Fig. 5). The predicted total event BFO dose is added to the section “Space Weather Condition” of the flight note (Hu et al., 2020), along with the issue time. For events with multiple predictions, the updated BFO doses as well as the issue times are appended. After the prediction finishes, a text “UMASEP proton intensity forecasting is now clear” is appended, while all predictions are displayed in the flight note to guide operations till the end of the event. The change of SPE status and triggering of the organ dose calculation are controlled by the HERA readings (Hu et al., 2020), so all other functions of original ARRT are not impacted by the addition of UMASEP-100 dose projection module.

## 6 Advantages of UMASEP-100 dose projection in ARRT

Table 3 lists the time parameters and dose results of the 41 hit events with UMASEP-100, calculated with ARRT 2.0. ARRT onset time for each event is determined by comparing the HERA dose rates with the background dose rate, which is calculated by checking and confirming that no SPE is in progress before the onset (Hu et al., 2020). The peak time is determined by visually checking with the highest dose rate after the onset of each event, and the UMASEP forecasted doses are obtained by using the linear fit formula for UMASEP-100 flux-dose correlation (Fig. 3). As UMASEP-100 predictions have a lower limit for the forecasted proton flux (i.e., 1.63 pfu), the forecasted BFO doses have a lower limit of 1.83 mGy-Eq (Table 3).

ARRT BFO doses are calculated with the ARRT organ dose algorithm, which has been described in detail in a previous paper (Mertens et al., 2018), involving the following four major steps:

1. Generate a database of silicon doses at vehicle dosimeter locations and organ doses at the normal crew seat locations as well as the crew locations inside the storm shelter, for 65 historical events with known total spectra.
2. Find the event in database that minimizes the differences between measured and database averaged dose in silicon, whose spectrum thus best matches the spectral shape of the real-time vehicle radiation environment.

3. Find the optimal scaling parameters between the vehicle dosimeter measurements and the precomputed absorbed dose in silicon at the dosimeter locations for the selected event in the historical SPE database.
4. Apply the scaling parameters to the database of organ doses to obtain real-time organ doses at the normal and storm shelter crew locations.

The measured dose rates are pre-calculated HERA dose rates using the same calibrated GOES data set and transport code HZETRN2015 to derive the flux-dose formula. However, the BFO doses in Table 1 are calculated from transport code, while those in Table 3 are from the ARRT algorithm, but both are for female astronaut at seat 1 (Hu et al., 2020).

The differences of UMASEP-100 warning times and ARRT onset times of all hit events and significant events (BFO doses > 5 mGy-Eq) are shown in Figure 6. For all 41 hit events, the average warning time is 59 min, close to that of 1 h and 6 min for v1.3 (Núñez, 2015). For a couple of events, the UMASEP issue times are later than the ARRT onset times; and for more events, the warning times are just 5–10 min earlier than the ARRT onset times (Fig. 6, left). For the 9 significant events, the average warning time reduces to 14 min, with 6 events within  $\pm 5$  min and 1 event 10 min earlier (Fig. 6, right). For the 4 most significant events with BFO doses > 17 mGy-Eq (2000-07-14, 2000-11-08, 2001-11-04, 2003-10-28), the warning times are -5, 5, -5, and 5 min, respectively (Table 3). It appears that the capability of UMASEP-100 to predict the onset time of significant events is limited, as the issue times are almost the same as those issued by the on-board dosimeters.

However, the warning time issued by UMASEP-100 is quite useful in space flight operations for the expected peaks of the events. Figure 7 shows the warning times before the peaks for the 9 significant events, with an average 588 min and a minimum 75 min. In case of severe SPEs, if there is a possible risk to crew health, the crew may be asked to perform the Radiation Event Cabin Reconfiguration (RECR) protocol and even seek shelter in the storage bays if needed (Hu et al., 2020). The crew shelter assembly is estimated to take about 30 min, and the current flight rule for the time to issue the RECR command is when the highest dose rate of the 6 HERA units exceeds 75  $\mu\text{Gy}/\text{min}$  (A. S. Johnson and D. Laramore, private communication). Even for the well-known fast rising 2000-07-14 event, according to transport calculation and modeling, the highest HERA dose rate goes above 75  $\mu\text{Gy}/\text{min}$  at 11:20, which is 40 min after UMASEP-100 issue time, and 45 min after the ARRT onset time (Table 3). As the prediction of UMASEP-100 at the issue time includes the peak flux, which quantitatively correlates the total BFO dose of the event as discussed above, the UMASEP forecasting will give the FCT important information to make timely decision in contingent scenarios to mitigate radiation exposure.

Though the forecasted BFO doses of UMASEP-100 have a lower limit (1.83 mGy-Eq), i.e., it cannot accurately predict the doses of small events, it shows capability to discretize minor events from significant ones (Fig. 8, left). For most insignificant events (ARRT BFO dose < 5 mGy-Eq), the forecasted doses are either the lower limit (1.83 mGy-Eq) or close to it, with only one significant overestimation (10.00 vs 0.08 mGy-Eq for the 2006-12-14 event) (Table 3; Fig. 8, left). For the 9 significant events (BFO dose > 5 mGy-Eq), 4 predictions are close to



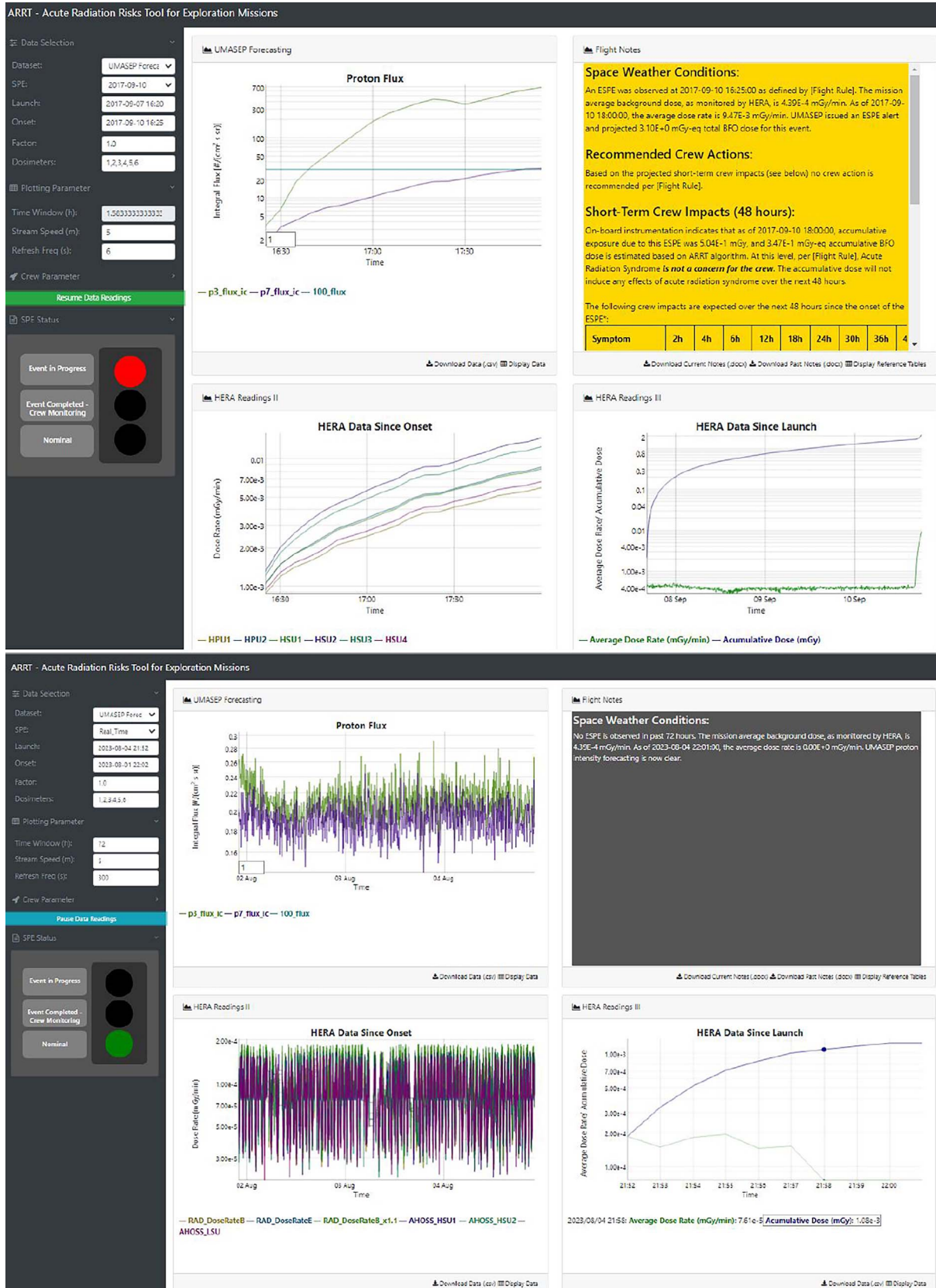


Figure 5. Interface update for ARRT 2.0, after integrating with UMASEP-100. The top panel is for historical events, and the bottom panel is for real time data stream. Detailed description of the interface elements can be found in ARRT 1.0 paper (Hu et al., 2020).

**Table 3.** Results of ARRT 2.0 for the hit events.

| SPE number | Event start time | UMASEP 3.4<br>issue time | ARRT 2.0<br>onset time | Peak<br>time | Forecasted BFO<br>dose (mGy-Eq) | ARRT BFO dose<br>(mGy-Eq)* |
|------------|------------------|--------------------------|------------------------|--------------|---------------------------------|----------------------------|
| 1          | 1997-11-06 12:45 | 12:30                    | 13:05                  | 15:15        | 2.18                            | 8.78 (1)                   |
| 2          | 1998-04-20 17:10 | 14:05                    | 20:20                  | 21/14:05     | 1.83                            | 1.55                       |
| 3          | 1998-05-02 14:05 | 14:00                    | 14:00                  | 15:20        | 2.47                            | 0.91                       |
| 4          | 1998-05-06 08:30 | 8:05                     | 8:35                   | 8:55         | 2.18                            | 0.20                       |
| 5          | 1998-08-24 23:10 | 22:50                    | 23:05                  | 25/1:00      | 1.99                            | 0.62                       |
| 6          | 1998-09-30 15:20 | 14:35                    | 14:35                  | 19:20        | 1.83                            | 0.45                       |
| 7          | 1998-11-14 07:55 | 6:55                     | 8:00                   | 9:50         | 1.89                            | 0.52                       |
| 8          | 2000-06-10 17:50 | 17:30                    | 17:50                  | 17:55        | 2.18                            | 0.08                       |
| 9          | 2000-07-14 10:40 | 10:40                    | 10:35                  | 11:55        | 39.00                           | 37.00 (2)                  |
| 10         | 2000-11-08 23:55 | 23:50                    | 23:55                  | 09/3:40      | 30.60                           | 22.50 (3)                  |
| 11         | 2000-11-24 17:20 | 17:15                    | 16:50                  | 18:00        | 1.83                            | 0.11                       |
| 12         | 2000-11-26 16:40 | 14:15                    | 17:00                  | 19:00        | 1.83                            | 0.13                       |
| 13         | 2001-04-03 01:20 | 02/20:00                 | 1:25                   | 7:45         | 1.99                            | 0.80                       |
| 14         | 2001-04-15 14:05 | 14:00                    | 14:00                  | 15:25        | 9.12                            | 10.20 (4)                  |
| 15         | 2001-09-24 14:40 | 12:45                    | 14:15                  | 25/7:55      | 1.99                            | 5.56 (5)                   |
| 16         | 2001-11-04 16:50 | 16:45                    | 16:40                  | 06/2:20      | 6.72                            | 17.00 (6)                  |
| 17         | 2001-11-22 22:50 | 22:10                    | 22:45                  | 24/5:50      | 1.83                            | 2.15                       |
| 18         | 2002-04-21 01:55 | 1:45                     | 1:55                   | 10:25        | 3.63                            | 3.58                       |
| 19         | 2002-08-22 03:40 | 2:50                     | 3:50                   | 5:10         | 1.83                            | 0.17                       |
| 20         | 2002-08-24 01:30 | 1:25                     | 1:25                   | 2:10         | 3.53                            | 1.46                       |
| 21         | 2003-10-28 11:45 | 11:35                    | 11:40                  | 29/00:15     | 11.80                           | 27.80 (7)                  |
| 22         | 2003-11-02 17:40 | 17:35                    | 17:40                  | 18:20        | 4.79                            | 1.55                       |
| 23         | 2003-11-05 05:10 | 04/21:20                 | 5:05                   | 5:05         | 1.83                            | 0.07                       |
| 24         | 2004-11-01 06:35 | 6:30                     | 6:45                   | 6:45         | 1.83                            | 0.11                       |
| 25         | 2004-11-10 03:20 | 3:25                     | 3:25                   | 3:30         | 2.18                            | 0.32                       |
| 26         | 2005-01-17 12:15 | 11:15                    | 11:40                  | 17:00        | 1.83                            | 3.02                       |
| 27         | 2005-06-16 21:25 | 20:40                    | 21:25                  | 23:45        | 2.02                            | 0.36                       |
| 28         | 2005-09-08 04:05 | 2:35                     | 3:25                   | 09/19:55     | 1.83                            | 4.79                       |
| 29         | 2006-12-07 01:15 | 0:50                     | 1:15                   | 12:00        | 1.83                            | 4.34                       |
| 30         | 2006-12-13 03:00 | 2:55                     | 3:00                   | 4:40         | 10.00                           | 6.16 (8)                   |
| 31         | 2006-12-14 22:55 | 22:45                    | 22:45                  | 23:35        | 10.00                           | 0.08                       |
| 32         | 2011-06-07 07:20 | 7:15                     | 8:00                   | 10:25        | 1.83                            | 0.67                       |
| 33         | 2011-08-04 05:10 | 4:40                     | 7:50                   | 7:55         | 1.83                            | 0.10                       |
| 34         | 2011-08-09 08:25 | 8:20                     | 8:25                   | 9:00         | 2.18                            | 0.13                       |
| 35         | 2012-01-23 04:45 | 4:40                     | 6:30                   | 7:50         | 1.83                            | 0.62                       |
| 36         | 2012-01-27 19:00 | 18:45                    | 19:30                  | 21:10        | 3.24                            | 1.02                       |
| 37         | 2012-03-07 04:05 | 4:00                     | 4:20                   | 15:35        | 1.83                            | 13.30 (9)                  |
| 38         | 2012-03-13 18:10 | 17:50                    | 18:35                  | 18:40        | 1.83                            | 0.08                       |
| 39         | 2012-05-17 02:00 | 2:00                     | 2:00                   | 2:00         | 2.69                            | 0.08                       |
| 40         | 2013-04-11 09:40 | 8:20                     | 10:15                  | 14:15        | 2.02                            | 0.32                       |
| 41         | 2013-05-22 14:55 | 14:05                    | 14:30                  | 18:50        | 1.89                            | 1.02                       |

\* 9 significant events with BFO doses > 5 mGy-Eq are denoted with numbers in brackets.

ARRT results (events 2, 3, 4, and 8 in Fig. 8, right), 2 predictions are approximately half of ARRT results (events 6 and 7), and 3 forecasted doses are just the lower limit (events 4 and 8) or near the limit (event 1). Together with 1 missed significant event, the failure rate of UMASEP-100 dose prediction for significant events during 1997–2013 is about 40%, indicating significant events forecasting cannot rely only on UMASEP-100 but need work together with other SPE forecasting tools (Whitman et al., 2022). Nevertheless, for the 32 hit insignificant events, this model correctly predicts 31 event doses in the range of the lower limit, with a success rate 97%. The capability to distinguish minor events from significant ones is important in space flight operation, as false alarms at an unacceptably high rate will cause disruptions for space activities.

After 2013, only 4 ESPEs occurred at the time of this writing, with 1 significant (2017-09-10) and 3 minor (2021-10-28, 2022-01-20 and 2022-03-28). UMASEP-100 v3.4 predicts all, with warning times for onset 5, –5, –15, and –15 min, respectively, compared with onsets determined by ARRT. The warning time for the peak of the significant 2017-09-10 event is 360 min. The dose rates of HERA units never reach 75  $\mu$ Gy/min, i.e., no RECR recommendation would be issued according to the flight rule. However, the total BFO dose for a female astronaut at seat 1 is 11.50 mGy-Eq, according to ARRT 1.0 algorithm. ARRT 2.0 initially predicts the BFO dose 4.90 mGy-Eq, then modifies to 5.17 mGy-Eq 5 min later. Though the forecasted dose is about a half, the prediction correctly distinguishes it as a significant event. For the 3 minor events, ARRT 2.0 also correctly predicts

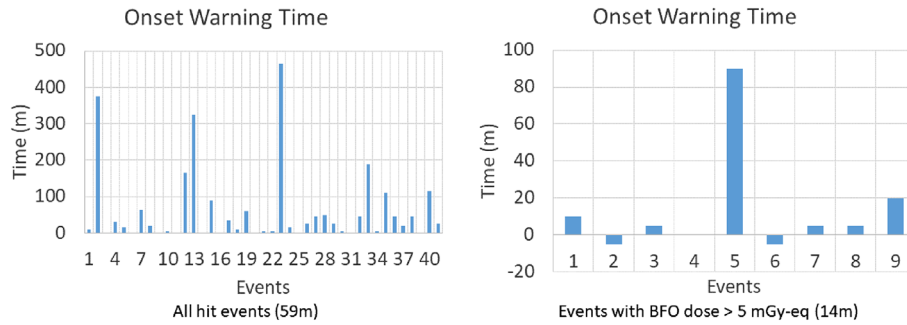


**Figure 6.** Warning times by UMASEP-100 for the onsets of events as detected by ARRT. The average warning time for all hit events is 59 min (left), and for significant events is 14 min (right).

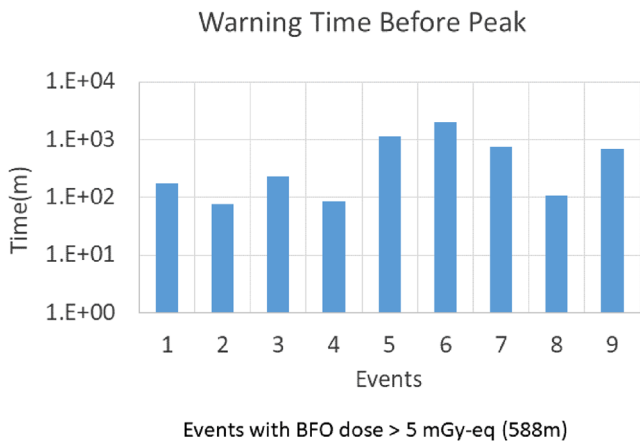


**Figure 7.** Warning times by UMASEP-100 before the peaks of 9 significant events (BFO doses  $> 5$  mGy-Eq).

all BFO doses at the lower limit, i.e., 1.83 mGy-Eq, while ARRT BFO doses are 1.72, 0.18, and 0.16 mGy-Eq, respectively.

## 7 Validation of ARRT organ dose calculation algorithm

The ARRT algorithm to calculate organ doses from onboard dosimeter measurements has been validated with the October 1989 event before (Mertens et al., 2018). Assuming an isotropic distribution of SPE protons, it was found that the differences are within 2% between the total organ doses predicted by this algorithm and those calculated from the original spectrum of this event, and the uncertainty of organ dose rates is on the order of 25–35% for the 329 time intervals (30 min; Mertens et al., 2018). This SPE is known as the most severe event with long duration of high fluxes of energetic protons in space era. In ARRT 2.0, a set of events with impacts from minor to significant during 1997–2022 can be used to check if the ARRT algorithm can accurately calculate total BFO doses from onboard dosimeter measurements.

The linear fitting in Figure 9 (left) shows the overall matching between the ARRT simulated BFO doses and transport calculated BFO doses for events during 1997–2022, with doses varying between 0.03 and 39.40 mGy-Eq (Tables 1 and 3). The average relative deviation ( $|\text{ARRT dose} - \text{transport}$

dose/transport dose) is 0.60 for 51 events (Fig. 9, left). For the 11 significant events (BFO dose  $> 5$  mGy-Eq), the matching is much better with an average deviation of 0.06 and a maximum deviation of 0.27. For the 40 minor events (Fig. 9, right), the average deviation is 0.74 with a maximum deviation of 2.62. It should be noted that the total doses from ARRT simulation are determined by comparing with the background dose rate of HERA, where a factor of 2.0 is used, while those from transport calculation are determined by comparing with the background BFO dose rate, where a factor 1.5 is used; therefore, most events do not have the same onset and ending times as detected by the two different methods (note that both factors were determined through prior testing). However, large events usually have long durations, the differences of onsets and endings are usually small, and the differences in calculated doses make small contributions to accumulative doses; small events are opposite in all these aspects. It can be ascertained that, for significant events, the results of ARRT algorithm are close to that by direct transport calculation, but for minor events, such as the proton flux elevation during the Artemis I passage of the Van Allen belt (Fig. 1), the ARRT simulated doses may be less reliable. When using ARRT for mission operations, the emphasis should be on predicting impacts of large events, where mitigation steps would be implemented; therefore, this compromised accuracy for predictions of smaller events is not of a great concern.

## 8 Conclusions and further work

This work reports an upgrade of ARRT by integrating with an established SEP forecasting model UMASEP-100, which makes real-time predictions of the time interval within which the  $>100$  MeV proton flux is expected to surpass 1 pfu and the intensity of the first 3 h of the event. Using a recently calibrated GOES recorded proton fluxes during 1994–2013, we do transport calculation to obtain total BFO doses of the events for astronauts inside Orion MPCV and apply the newest UMASEP-100 model to derive the proton fluxes of the first 3 h of these events. With these results, a formula of flux-dose correlation is identified and is validated with other events not in this period. With this formula, a module is added to ARRT to link UMASEP-100 outputs for historical events and real-time forecasting, so that the total BFO dose of an event can be displayed in the flight note whenever UMASEP-100 model issues a warning.

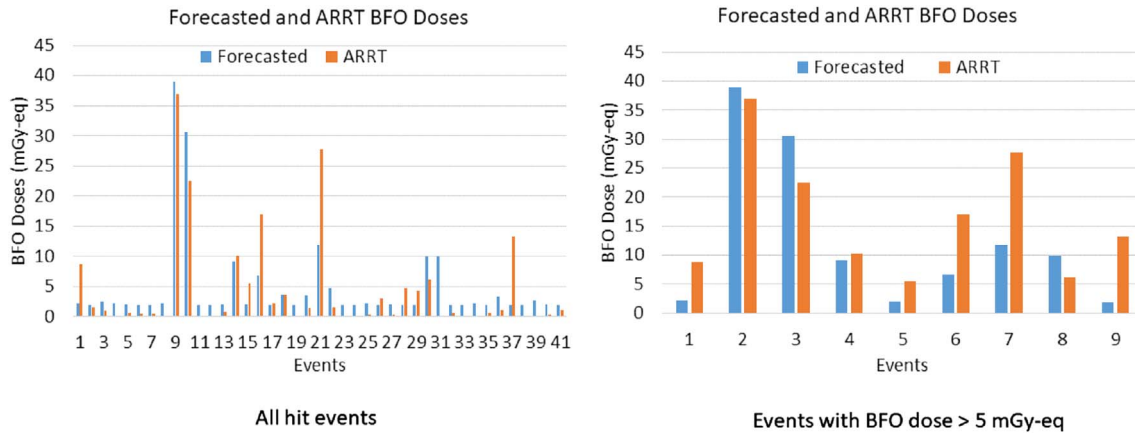


**Figure 8.** Comparison of forecasted BFO doses by UMASEP-100 and calculated BFO doses by ARRT for all hit events (left) and for significant events (right).

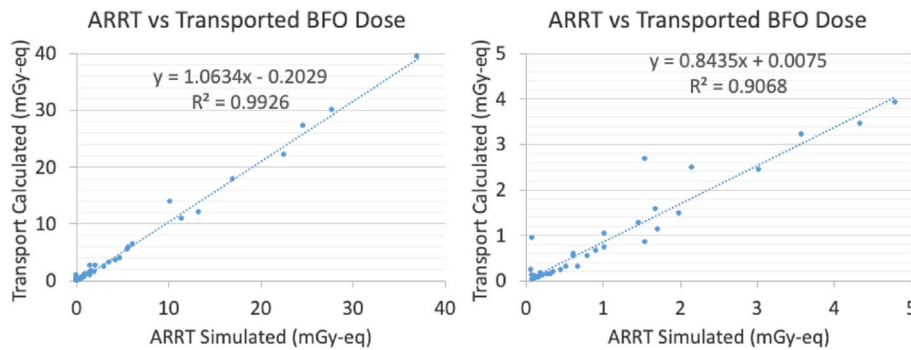


**Figure 9.** Correlation between ARRT simulated BFO doses and transport calculated BFO doses for events during 1997–2022 (left), and for minor events (<5 mGy-Eq) among them (right).

Tested with events during 1994–2022, the UMASEP forecasting on the onset does not demonstrate much advantage as the predicted times are almost the same as those detected by onboard dosimeters, nevertheless, for significant events with BFO dose > 5 mGy-Eq, it shows the warning times before the peaks with an average 588 min and a minimum 75 min. Together with the total BFO dose of the event, the UMASEP forecasting will give the FCT important information to make timely decision in contingency scenarios to mitigate radiation exposure. In addition, ARRT 2.0 shows the capability to distinguish minor events from significant ones, which is also important in space flight operation to avoid false alarms that will cause disruptions for space activities.

An alternative approach to apply UMASEP set of models in space flight operation is to combine the forecasted proton fluencies at specific energies so that the predicted proton spectrum can be used to estimate organ doses via transport calculation. UMASEP-10 (Núñez, 2011; Núñez, 2022), UMASEP-30, UMASEP-50, UMASEP-100 (Núñez, 2015), and HESPERIA UMASEP-500 (Núñez et al., 2017) have been deployed at CCMC and are running continuously in real time (<https://ccmc.gsfc.nasa.gov/models/UMASEP-v3/>), the outputs of which can be retrieved the same way as in this work and coupled with energetic particle transport code such as HZETRN (Slaba et al., 2016; Wilson et al., 2016) for real time dose

calculation and risks analysis. The benefits of this approach include more advanced warning time, higher probability of detection (POD) and lower false alarm ratio (FAR) (Núñez, 2015), as well as much wider range of application as spacecraft is not restricted to Orion MPCV and any kind of space flight missions that UMASEP models are applicable can be simulated. A following paper will describe this approach and software implement. In addition, a new submodel, called the SEP Peak Prediction submodel (SPP-100), is under development, which consists of both new empirical and machine learning elements. In real-time, when UMASEP-100 predicts the occurrence of a >100 MeV SEP event (via the WCP and PCP submodels), the SPP-100 submodel will be triggered to predict the expected >100 MeV SEP peak flux, which is better correlated with crew dose as demonstrated in this work.

The development of ARRT algorithm (Mertens et al., 2018) and all transport calculations of this work assumed the SEP proton flux is isotropic, i.e., the flux is the same from all directions during the event. For large SEP events, especially those GLEs with hard spectra, the solar particle flux travelling along the interplanetary magnetic field can be well collimated giving rise to an anisotropic particle flux distribution in the initial phase of the events (Shea & Smart, 2012). The doses calculated by transport code with isotropic assumption can be significantly overestimated in these scenarios. Thus, caution is needed to interpret



the modeled crew doses for anisotropic events. Current flight rules for Artemis missions are based on onboard dosimeters' readings, as their measurements are based on counting of the particles directly, not dependent upon the directional characteristics of particle flux outside of the vehicle (Stoffle et al., 2023).

### Acknowledgements

This work was supported by KBR Human Health and Performance Contract (HHPC) NNJ15HK11B. The authors appreciate Dr. Kathryn Whitman (NASA JSC) for sharing code to retrieve GOES 16 integral flux from the ISWA – HAPI Server at NASA Goddard Space Flight Center (GSFC) (<https://iswa.gsfc.nasa.gov/IswaSystemWebApp/hapi/>), and are grateful for comments and suggestions from Dr. Luke Stegeman and Dr. Kathryn Whitman (NASA JSC). The editor thanks Fan Lei and Ondřej Ploc for their assistance in evaluating this paper.

### References

- Cucinotta FA, Hu S, Schwadron NA, Kozarev K, Townsend LW, Kim MHY. 2010. Space radiation risk limits and Earth-Moon-Mars environmental models. *Space Weather* **8**: S00E09. <https://doi.org/10.1029/2010SW000572>.
- Hu S, Cucinotta FA. 2011. Characterization of the radiation-damaged precursor cells in bone marrow based on modeling of the peripheral blood granulocytes response. *Health Phys* **101**(1): 67–78. <https://doi.org/10.1097/HP.0b013e31820dba65>.
- Hu S, Kim MHY, McClellan GE, Cucinotta FA. 2009. Modeling the acute health effects of astronauts from exposure to large solar particle events. *Health Phys* **96**(4): 1–12. <https://doi.org/10.1097/01.HP.0000339020.92837.61>.
- Hu S, Monadjemi S, Barzilla JE, Semones E. 2020. ARRT development for the upcoming human exploration missions. *Space Weather* **18**: e2020SW002586. <https://doi.org/10.1029/2020SW002586>.
- Hu S, Semones E. 2022a. Calibration of the GOES 6–16 high-energy proton detectors based on modelling of ground level enhancement energy spectra. *J Space Weather Space Clim* **12**: 5. <https://doi.org/10.1051/swsc/2022003>.
- Hu S, Semones E. 2022b. Multi-source calibrated GOES dataset and solar radiation environment model update. NASA/TP-20220008181. <https://ntrs.nasa.gov/citations/20220008181>.
- Hu S, Smirnova OA, Cucinotta FA. 2012. A biomathematical model of lymphopoiesis following severe radiation accidents – potential use for dose assessment. *Health Phys* **102**(4): 425–436. <https://doi.org/10.1097/HP.0b013e318240593d>.
- Hu S, Zeitlin C, Atwell W, Fry D, Barzilla JE, Semones E. 2016. Segmental interpolating spectra for solar particle events and in situ validation. *Space Weather* **14**: 742–753. <https://doi.org/10.1002/2016SW001476>.
- Mertens CJ, Slaba TC, Hu S. 2018. Active dosimeter-based estimate of astronaut acute radiation risk for real-time solar energetic particle events. *Space Weather* **16**: 1291–1316. <https://doi.org/10.1029/2018SW001971>.
- NASA. 2023. NASA spaceflight human system standard. Vol. 1, Revision C: Crew health. [https://standards.nasa.gov/standard/NASA/NASA-STD-3001\\_VOL\\_1](https://standards.nasa.gov/standard/NASA/NASA-STD-3001_VOL_1) (accessed November 13, 2024).
- National Academies of Sciences, Engineering, and Medicine. 2021. *Space radiation and astronaut health: managing and communicating cancer risks*. The National Academies Press, Washington, DC. <https://doi.org/10.17226/26155>.
- National Council on Radiation Protection. 2000. National council on radiation protection and measurements: radiation protection guidance for activities in low-Earth orbit (NCRP Rep. No. 132): National Council on Radiation Protection and Measurements.
- Núñez M. 2011. Predicting solar energetic proton events ( $E > 10$  MeV). *Space Weather* **9**: S07003. <https://doi.org/10.1029/2010SW000640>.
- Núñez M. 2015. Real-time prediction of the occurrence and intensity of the first hours of  $>100$  MeV solar energetic proton events. *Space Weather* **13**: 807–819. <https://doi.org/10.1002/2015SW001256>.
- Núñez M. 2022. Evaluation of the UMASEP-10 version 2 tool for predicting all  $>10$  MeV SEP events of solar cycles 22, 23 and 24. *Universe* **8**: 35. <https://doi.org/10.3390/universe8010035>.
- Núñez M, Reyes-Santiago PJ, Malandraki OE. 2017. Real-time prediction of the occurrence of GLE events. *Space Weather* **15**: 861–873. <https://doi.org/10.1002/2017SW001605>.
- Raukunen O, Vainio R, Tylka AJ, Dietrich WF, Jiggins P, Heynderickx D, et al. 2018. Two solar proton fluence models based on ground level enhancement observations. *J Space Weather Space Clim* **8**: A04. <https://doi.org/10.1051/swsc/2017031>.
- Shea MA, Smart DF. 2012. Space weather and the ground-level solar proton events of the 23rd solar cycle. *Space Sci Rev* **171**(1): 161–188. <https://doi.org/10.1007/s11214-012-9923-z>.
- Slaba TC, Qualls GD, Cloudsley MS, Blattning SR, Walker SA, Simonsen LC. 2010. Utilization of CAM, CAF, MAX, and FAX for space radiation analyses using HZETRN. *Adv Space Res* **45**(7): 866–883. <https://doi.org/10.1016/j.asr.2009.08.017>.
- Slaba TC, Wilson JW, Badavi FF, Reddell BD, Bahadori AA. 2016. Solar proton exposure of an ICRU sphere within a complex structure: ray-trace geometry. *Life Sci Space Res* **9**: 77–83. <https://doi.org/10.1016/j.lssr.2016.05.001>.
- Stoffle NN, Campbell-Ricketts T, Castro A, Gaza R, Zeitlin C, George S, Abdelmelek M, Schram A. 2023. HERA: a timepix-based radiation detection system for exploration-class space missions. *Life Sci Space Res* **39**: 59–66. <https://doi.org/10.1016/j.lssr.2023.03.004>.
- Whitman K, Egeland R, Richardson IG, Allison C, Quinn P, et al. 2022. Review of solar energetic particle prediction models. *Adv Space Res* **72**(12): 5161–5242. <https://doi.org/10.1016/j.asr.2022.08.006>.
- Wilson JW, Denn FM. 1976. Preliminary analysis of the implications of natural radiations on geostationary operations. NASA-TN-D-8290. <https://ntrs.nasa.gov/citations/19760026032>.
- Wilson JW, Slaba TC, Badavi FF, Reddell BD, Bahadori AA. 2016. Solar proton exposure of an ICRU sphere within a complex structure: combinatorial geometry. *Life Sci Space Res* **9**: 69–76. <https://doi.org/10.1016/j.lssr.2016.05.002>.

**Cite this article as:** Hu S, Barzilla JE, Núñez M & Semones E. 2025. Real-time dose prediction for Artemis missions. *J. Space Weather Space Clim.* **15**, 1. <https://doi.org/10.1051/swsc/2024037>.